Canceling actions involves a race between basal ganglia pathways

Robert Schmidt[1], Daniel K Leventhal[2], Nicolas Mallet[1,3], Fujun Chen[1] & Joshua D Berke[1]

Salient cues can prompt the rapid interruption of planned actions. It has been proposed that fast, reactive behavioral inhibition involves specific basal ganglia pathways, and we tested this by comparing activity in multiple rat basal ganglia structures during performance of a stop-signal task. Subthalamic nucleus (STN) neurons exhibited low-latency responses to 'Stop' cues, irrespective of whether actions were canceled or not. By contrast, neurons downstream in the substantia nigra pars reticulata (SNr) only responded to Stop cues in trials with successful cancellation. Recordings and simulations together indicate that this sensorimotor gating arises from the relative timing of two distinct inputs to neurons in the SNr dorsolateral 'core' subregion: cue-related excitation from STN and movement-related inhibition from striatum. Our results support race models of action cancellation, with stopping requiring Stop-cue information to be transmitted from STN to SNr before increased striatal input creates a point of no return.

The ability to suppress and cancel actions is a core component of cognitive control, and impairments in this ability contribute to impulsive and compulsive behaviors including drug addiction and attention-deficit hyperactivity disorder[1–5]. Action suppression is often assessed using the stop-signal task, which has been widely applied in both humans and experimental animals[3,6–8]. On most trials, subjects are given a 'Go' cue that prompts a specific, rapid movement. On the remaining trials the same Go cue is followed by a 'Stop' signal, indicating that the subjects should cancel that movement before it begins. The interval between Go and Stop cues is adjusted so that subjects sometimes succeed in stopping and sometimes fail in stopping. In general, stop-signal task performance is well described by theoretical models in which the Go and Stop cues respectively initiate stochastic go and stop processes that race for completion. The outcome of this race determines whether stopping is successful[3,4].

Extensive evidence for involvement of the basal ganglia in action suppression comes from pharmacological manipulations[9,10], lesions[6,11], stimulation[12,13], imaging[1,14] and computational modeling[2,15]. It has been proposed that the conceptual race between go and stop processes corresponds to a literal race between distinct neural pathways[1], converging on basal ganglia output nuclei that provide tonic inhibition of actions[16,17]. Specifically, striatal 'direct' pathway neurons are thought to promote movements (go) by inhibiting SNr, and STN neurons serve as a brake on behavior (stop) by exciting the same SNr cells[2,18] (**Fig. 1a**). Here we tested this hypothesis by comparing the fine timing of activity in each basal ganglia structure. Our results support the basic notion of a race between go and stop processes that initially evolve in separate neural circuits, and also provide evidence for multiple basal ganglia mechanisms in behavioral inhibition[14,19].

RESULTS

To assess the correspondence between distinct basal ganglia pathways and hypothesized cognitive processes, we applied the high spatiotemporal resolution of single-unit electrophysiology to a rat stop-signal task based around our prior decision-making studies[20,21] (**Fig. 1** and **Supplementary Table 1**). We trained each rat to place its nose in a central port until the onset of a Go cue (1-kHz or 4-kHz tone) that directed a brief lateral head movement (to the left or the right; **Supplementary Video 1**). On 30% of trials, this Go tone was followed by a Stop cue (white noise), instructing that the rat should stay in the central port (**Fig. 1b,c**). For both Go trials and Stop trials, we rewarded correct performance by delivery of a sugar pellet. As typically observed for stop-signal tasks, reaction times for Failed Stop trials corresponded to the faster portion of the reaction-time distribution in Go trials (**Fig. 1d**). This is consistent with race models: when the go process happens more quickly, a stop process is less likely to suppress behavior.

For our first set of recordings (experiment 1), four well-trained subjects received tetrode implants that simultaneously targeted sensorimotor striatum, STN, globus pallidus (corresponding to globus pallidus pars externa in primates) and SNr[21]. We isolated spikes from individual neurons during task performance, from each brain region (for anatomical locations, see **Supplementary Fig. 1**). A challenge when studying behavioral inhibition is to disentangle neural activity specifically linked to stopping, rather than going. To do this, we followed a latency-matching procedure[22,23] (Online Methods), which exploits the similarity in reaction times, and thus presumably the go process, between Failed Stop trials and Fast Go trials. We compared the firing rate of each neuron between these trial types, and between Correct Stop trials and Slow Go trials. We then assessed the fraction of each neuronal

Figure 1 Task events and behavior. (**a**) Simplified scheme of neural circuitry under investigation during the stop-signal task. Projections from striatum (STR) and STN converge on SNr, which provides tonic inhibition of motor output. GP, globus pallidus. (**b**) Configuration of the operant chamber with five nose ports on one side and a food port on the opposite side. Entry into any port is detected by breaks of photodiode beam (red dashed lines). (**c**) Task events in Go trials and Stop trials are shown in sequence from left to right. Thick bars indicate occurrence of sensory cues ('audio' and 'house light') and rat position in center and side ports. Reaction time (RT) is measured between onset of Go cue and onset of movement (that is, 'nose out' of the center port). Movement time (MT) is the time it takes the rat to go from the center port to the side port. In Stop trials, the stop-signal delay (SSD) is the time between onset of Go cue and onset of Stop cue. (**d**) Reaction time distributions for experiment 1 (rats 10–13, top to bottom). Correct Go trials are shown in blue, and Failed Stop trials in purple. Note that Failed Stop trials have similar reaction times to the faster part of the distribution for Go trials.
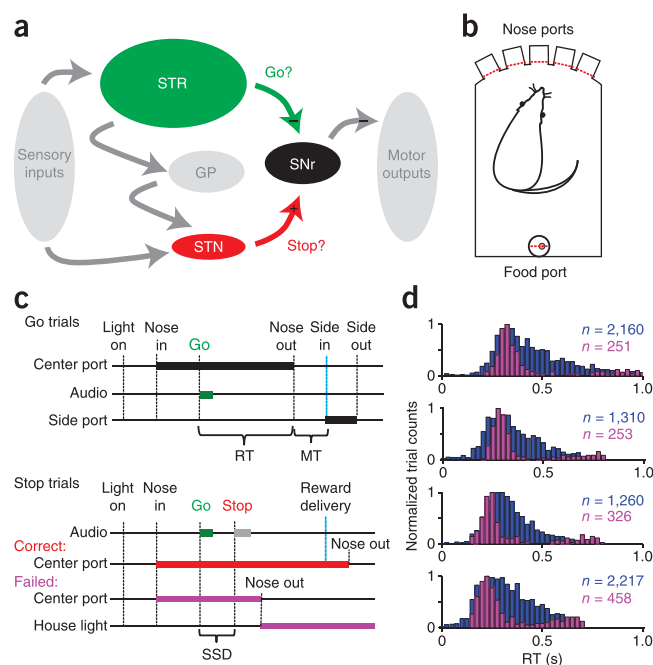

population that exhibited significant ($P < 0.05$; shuffle test) differences at each moment in time (**Fig. 2a** and **Supplementary Fig. 2**).

Striatal neurons showed little or no fast population-level response to the Stop signal. In contrast, both STN and SNr contained a significant proportion of neurons with rapid responses to the Stop signal ($P < 0.05$, binomial test; **Fig. 2a,b**). For STN, this proportion was similar for Correct and Failed Stop trials (see **Supplementary Fig. 2** for a comparison between these trial types) and thus resembled a 'sensory'-like population response to the Stop cue. However, for SNr, the Stop cue evoked a fast activity change only in Correct Stop and not

in Failed Stop trials (**Fig. 2a**). Thus, although the activity in STN was consistent with a sensory response, activity in SNr instead reflected the behavioral outcome on each trial.

Figure 2 Distinct processing of the Stop cue across basal ganglia components. (**a**) Fraction of neurons whose firing rate significantly differed between the trial types under comparison, for indicated brain areas during contralateral trials. To screen for stop-related activity, we compared Correct Stop trials with Slow Go trials (top), and Failed Stop trials with Fast Go trials (bottom). For example, movement-related activity was very similar on Fast Go and Failed Stop trials, so it does not show up in this comparison. Activity is aligned to onset of the Stop cue (or for Go trials, the point at which the Stop cue would have been presented had it been a Stop trial). Upward and downward bars denote the fraction of units that fired more on Stop and Go trials, respectively. Filled bars indicate times when this fraction significantly exceeded chance level (binomial test; $P < 0.05$ with pale bars uncorrected and dark bars corrected for multiple comparisons; horizontal gray lines mark these respective significance thresholds). In this latency-matched analysis, the proportions of STN neurons with fast Stop cue responses were similar in Correct Stop and Failed Stop trials (for the two STN bins just after the onset of Stop cue; $P = 0.17$ and 0.21, shuffle test). By contrast, these proportions were significantly different for SNr (for the two filled red SNr bins, $P = 0.008$ and 0.005, shuffle test). (**b**) Examples of individual neuron activity in STN and SNr during Go trials in the four relevant trial types as indicated (both ipsilateral and contralateral movements are shown). The STN unit showed a fast, transient increase in activity after the Stop cue in both Correct and Failed Stop trials. On Correct Stop trials, the SNr unit also exhibited a fast increase in firing, and no movement-linked pause. By contrast, on Failed Stop trials, the SNr unit simply showed a movement-linked decrease in firing rate and no response to the Stop cue, very similar to Fast Go trials.
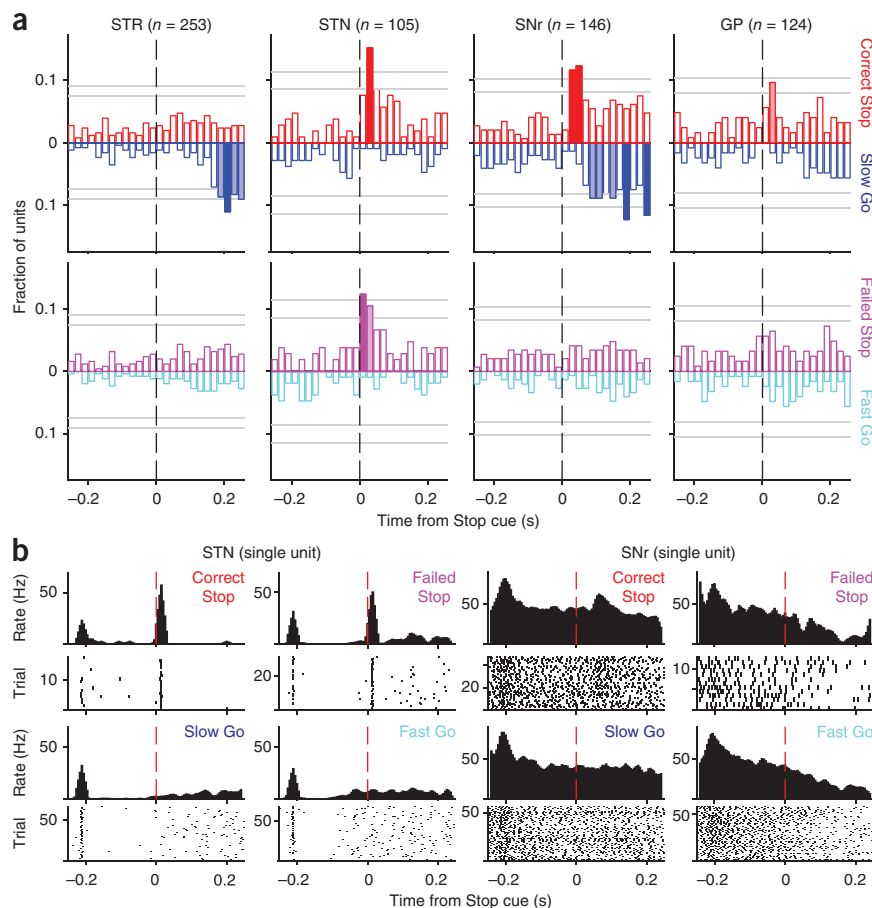
Figure 3 Stop cues increase firing in STN before SNr. (**a**) Firing rate time courses for the neuronal subpopulations that distinguish Stop from Go trials (in contralateral trials; **Fig. 2** and Online Methods). Colored lines show the mean (± s.e.m.) z-score of the firing rate across units (rat breakdown: 11 and 16 STN units from rats 10 and 11, respectively; 14, 2 and 2 SNr units from rats 10, 12 and 13, respectively; see **Supplementary Table 1**). Horizontal colored bars at the top of each panel indicate times with significantly different Stop versus Go firing rates (shuffle test, $P < 0.05$, corrected for multiple comparisons). Vertical gray bars show SSRTs for the corresponding recording sessions. (**b**) Comparison of Stop cue response latencies for the same STN (black) and SNr (green) units (top, Correct Stop trials; bottom, Failed Stop trials). To aid comparison, baselines are shifted so that lowest activity is in all cases at zero. Vertical dashed lines indicate latency of peak response (STN, 15 ms; SNr, 36 ms); red line marks shortest SSRT. Insets, distributions of single unit response latencies. (**c**) Peak Stop cue response amplitudes for individual neurons in Correct versus Failed Stop trials (top, STN; bottom SNr; gray lines ± s.e.m.). P values were derived from shuffle tests.
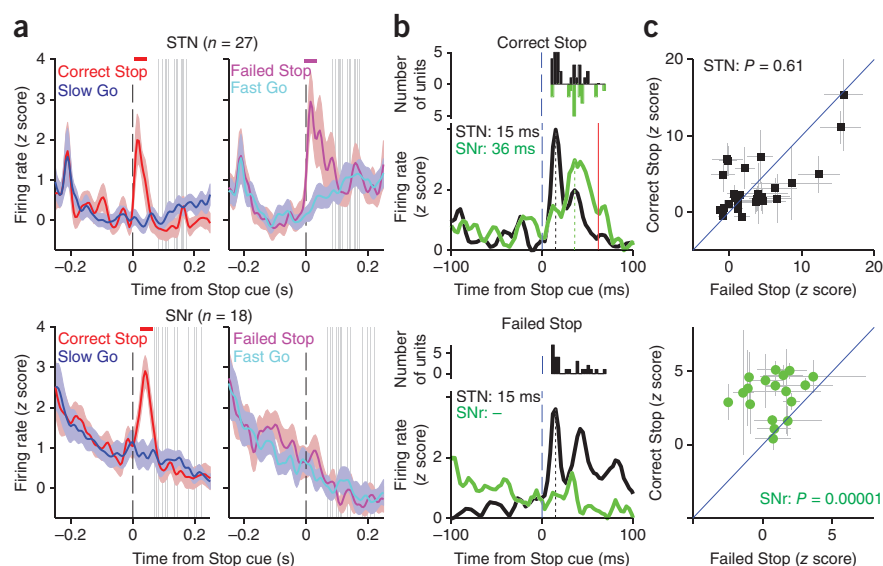
Our globus pallidus recordings did not yield such unambiguous results. Although the initial screen indicated that some neurons may selectively respond for Correct Stops (**Fig. 2a**), the direct comparison did not confirm a selective globus pallidus response in Correct Stop rather than in Failed Stop trials (**Supplementary Fig. 2**). We therefore focused on STN and SNr next.

We examined the time course of activity in these stop-related STN and SNr neurons. STN neurons responded to the onset of the Stop cue with transiently increased firing (**Fig. 3a**) that in some cases took the form of just a single, precisely timed extra spike (**Fig. 2b**). These STN increases had consistently very low latencies (peak response ~15 ms; **Fig. 3b**; see ref. 24 for similarly low STN latencies) that were not different between Correct and Failed Stop trials ($P = 0.41$, paired t-test; **Fig. 3b**). The magnitude of the peak STN response exhibited no consistent preference for Correct Stop versus Failed Stop trials (**Fig. 3c**). SNr neurons also increased firing in response to the Stop cue (**Fig. 3a**)

but with a longer latency (peak response at ~36 ms; **Fig. 3b**; $P = 0.004$ comparing STN to SNr latencies, one-sided Kolmogorov-Smirnov test) and preferentially on Correct Stop trials (**Fig. 3c**). We observed this latency difference even when we restricted the analysis to units recorded in the same session ($n = 15$ pairs; STN cells preceded SNr cells by an average of 13.6 ms, $P = 0.041$, shuffle test). All SNr neurons that responded to the Stop cue on Correct Stop trials did so before the stop-signal reaction time (SSRT; **Fig. 3a**), a standard, inferred behavioral measure for how quick a process must be to influence stopping performance[3,4,7]. Thus, SNr activity not only distinguished between Correct and Failed Stop trials, it did so quickly enough to affect the trial outcome.

Most of the SNr units with fast responses to the Stop cue (10/18) also markedly decreased their activity beginning just before movement (**Supplementary Fig. 3**). This suggests that the Stop cue may not alter SNr activity globally, but rather have a selective influence over

Figure 4 An SNr hotspot for Stop cue responses. (**a**) Example of a silicon probe recording from SNr. Tips of the eight probe shanks were coated in DiO (green) for histological visualization. One tip is visible here (the others were more anterior and posterior). Dashed line marks SNr boundary. (**b**) Reconstructed locations of SNr single units from all nine rats, on SNr coronal atlas boundaries[51] (Online Methods). Neurons showing significant ($P < 0.05$; shuffle test) differences between Correct and Failed Stop trials (20–100 ms after Stop cue in either ipsilateral or contralateral trials) are shown in red; others are in cyan. Numbers indicate approximate anterior to posterior coordinate relative to bregma. (**c**) Functional map obtained by stacking atlas sections. Note the dorsolateral cluster of outcome-dependent SNr units (10, 11 and 3 units from rats 11, 15 and 18, respectively; **Supplementary Table 1**). This cluster was observed when either ipsi- or contralateral movements had to be stopped and also in latency-matched control comparisons (**Supplementary Fig. 4a–d**). (**d**) Representative unit from the hotspot (from rat 15, marked by white 'x' in **b**) showing similar activity patterns to SNr units from experiment 1.
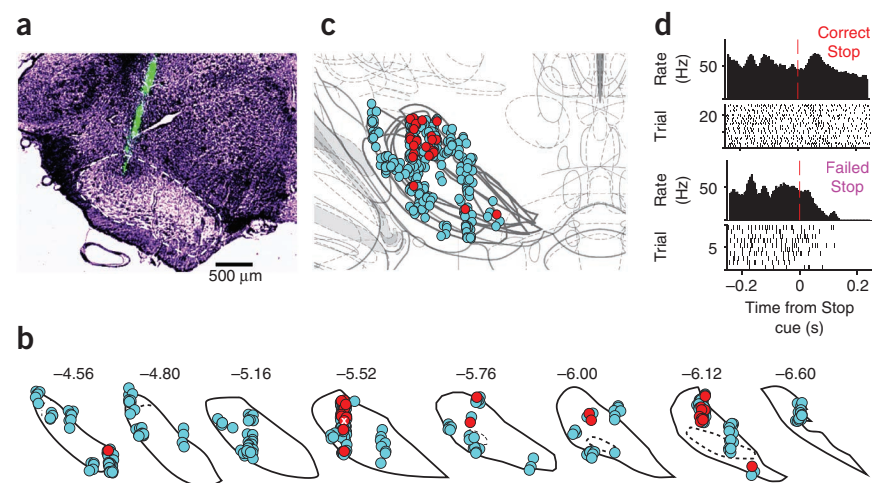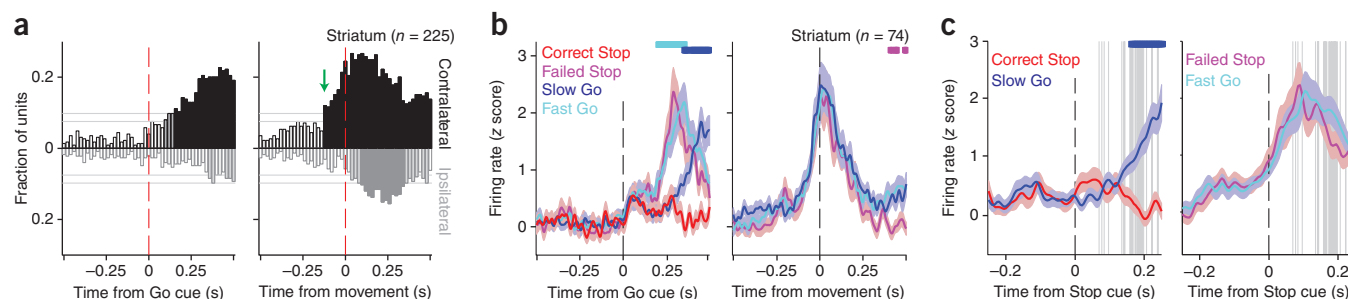
Figure 5 Variable timing of a striatal go process critically determines whether stopping is successful. (**a**) Fractions of striatal units distinguishing between contra- and ipsilateral movements, at each time point during Go trials. Layout is as in **Figure 2**. On the right, black solid bars before the red dashed line indicate significant ($P < 0.05$, shuffle test) coding of movement direction before the onset of movement. The 74 units that contributed to these bars were considered potential contributors to a go process (rat breakdown: 5, 23, 11 and 35 units from rats 10–13, respectively; **Supplementary Table 1**). (**b**) Mean (± s.e.m.) firing rate z score for these 74 striatal units. Cyan bar at the top indicates times with significantly different firing rates on Fast versus Slow Go trials, blue bar indicates the same for Slow Go versus Correct Stop trials, and purple bar for Fast Go versus Failed Stop trials (shuffle test, $P < 0.05$, corrected for multiple comparisons). (**c**) Activity of the same striatal units aligned to the Stop cue. Note the different time scale than in **b**. Format is as in **Figure 3a**.

cells and subregions involved in controlling the movement that needs to be inhibited. We therefore recorded from a second set of subjects (experiment 2) using both high-density silicon probes (in three rats, **Fig. 4a**) and more tetrodes (in two rats) to target a wide range of SNr locations. Combining all SNr results together revealed a clear 'hotspot' of SNr cells that distinguished Correct Stop trials from Failed Stop trials, briefly after the Stop cue (**Fig. 4** and **Supplementary Fig. 4a–d**). This hotspot corresponds remarkably well to the SNr sensorimotor 'core' subregion that has been described in anatomical studies[25], located dorsolaterally and extended along the rostral-caudal axis. This subregion projects to specific parts of the superior colliculus involved in orienting movements[25,26], so the Stop signal influences activity in an SNr subregion that is likely critical for exerting fast behavioral control[27].

The distinct latencies of STN and SNr cue responses are consistent with stop information being conveyed along the STN-SNr pathway. Yet the selectivity of this transmission to Correct Stop trials suggests some form of gating mechanism. In other words, given that the glutamatergic STN cells spike on Failed Stop trials, why are SNr neurons not responsive to this input? The answer may lie in the movement-related firing-rate decreases of SNr neurons (**Supplementary Figs. 3 and 4e,f**). Such SNr firing pauses are well known from studies of eye and limb movements[27,28], and are thought to facilitate action through disinhibition of superior colliculus and other structures more directly linked to motor output[16,29]. SNr pauses are driven by increased firing of the GABAergic striatal direct pathway neurons[17,30], plausible participants in a go process.

To assess how striatal neurons may contribute to movement preparation and initiation, we looked for units that distinguish movement direction before onset of movement. We found an abrupt increase in contralateral coding starting ~140 ms before movements (**Fig. 5a**; see **Supplementary Fig. 5** for analyses of other brain regions). When we compared the activity of these direction-selective striatal neurons (74 cells) between different trial types, we observed a rapid acceleration of firing rate just before the onset of movement[31] (**Fig. 5b**) that followed the same trajectory for Fast Go, Slow Go and Failed Stop trials. Aligned on the earlier Go cue, this striatal activity remained very similar between Fast Go and Failed Stop trials but distinct to Slow Go and Correct Stop trials (**Fig. 5b**).

These results fit well with a simple race model, in which variability in the timing of a striatal-based go process determines the outcome

on Stop trials. On Failed Stop trials, movement-related striatal activity has already begun to increase by onset of Stop cue (**Fig. 5c** and **Supplementary Fig. 6**). This effect was particularly pronounced when examining individual presumed striatal projection neurons (**Supplementary Fig. 6b**). Therefore, the lack of SNr responses to the Stop cue on Failed Stop trials may be due to the early arrival of striatal GABAergic input, shunting away the effects of glutamatergic inputs from the STN.

To confirm the viability of this idea, we studied gating of the Stop cue responses in a simple integrate-and-fire model of an SNr neuron. This neuron received excitatory pulses, mimicking STN sensory responses to Stop cues, and (as in prior basal ganglia models[32,33]) this excitatory input was influenced by GABAergic inhibition[34,35] (Online Methods). For GABAergic input, we used the average striatal population activity during initiation of movement (**Fig. 5b**) to approximate real input patterns. We adjusted synaptic strengths of inhibitory and excitatory inputs to provide a good qualitative match with the cue-evoked increases and movement-related decreases in SNr firing.

A critical parameter in the model is the relative timing of excitation and inhibition. We defined Δ as the interval between the Stop cue onset cue and the point in the striatal output at which movements began on Go trials. If the Stop cue began long before initiation of movement (**Fig. 6a**; $\Delta = 200$ ms), striatal inhibition was low at that time and the Stop cue evoked a full response in the SNr cell. In contrast, if the Stop cue occurred only briefly before initiation of movement (**Fig. 6a**; $\Delta = 50$ ms), a high level of striatal inhibition suppressed the SNr cue response. A systematic variation of Δ in the behaviorally relevant range yielded a gating curve that quantified the model response to the Stop cue (**Fig. 6b,c**). The gating phenomenon required strong divisive inhibition, for example, through shunting inhibition, rather than simple summation of inhibitory and excitatory conductances (**Fig. 6c**). We then used the behavioral data of each rat to estimate the actual distribution of Δ for both Correct and Failed Stop trials (**Supplementary Fig. 7**). Then we could use these Δ distributions to calculate model firing rates for these trial types (**Fig. 6d**). Just as for real rat SNr cells, the model SNr cell selectively responded to the Stop cue in Correct Stop trials but not in Failed Stop trials. We conclude that the integration of distinct excitatory and inhibitory synaptic inputs by individual SNr neurons provides a straightforward, mechanistic account of how go and stop processes can 'race' in the brain.

Figure 6 Modeling sensorimotor gating in SNr neurons. (**a**) Model responses for two illustrative values of Δ, the interval between onset of Stop cue and onset of movement. Red and green lines indicate STN and striatal (STR) inputs to the SNr model, and blue line shows the output firing rate of the model SNr cell. Note the clear SNr response to the Stop cue with Δ = 200 ms but not with Δ = 50 ms. (**b**) SNr model responses to the Stop cue over a range of Δ. For small Δ, strong shunting inhibition from striatum prevents STN-evoked spiking to the Stop cue (white arrow). (**c**) Comparison between model output with and without the Stop cue, measured in the 50 ms after STN input reaches SNr (left). Enlarged view of the gray area (right), for the range of Δ where gating of Stop cue occurs. Red line is the same as on the left; other lines show the effects of different levels of shunting inhibition (low values of the reference current J correspond to strong divisive inhibition; Online Methods). In all cases the lines indicate the difference between model SNr firing rate with and without the Stop cue. Note that without shunting inhibition the model does not gate the Stop cue as observed in the experimental SNr data. (**d**) Model SNr output (colored lines) exhibits response to the Stop cue in Correct Stop trials (top) but not in Failed Stop trials (bottom). Failed and Correct Stop trials in the model are based on rat reaction time data

(**Supplementary Fig. 7**). Black histogram shows one example rat SNr cell for qualitative comparison to the model. Note that in the model, increased firing to the Stop cue response was always followed by a movement-related decrease as, for simplicity, we did not incorporate our observation that striatal output is subsequently suppressed on Correct Stop trials (**Fig. 5b,c**).
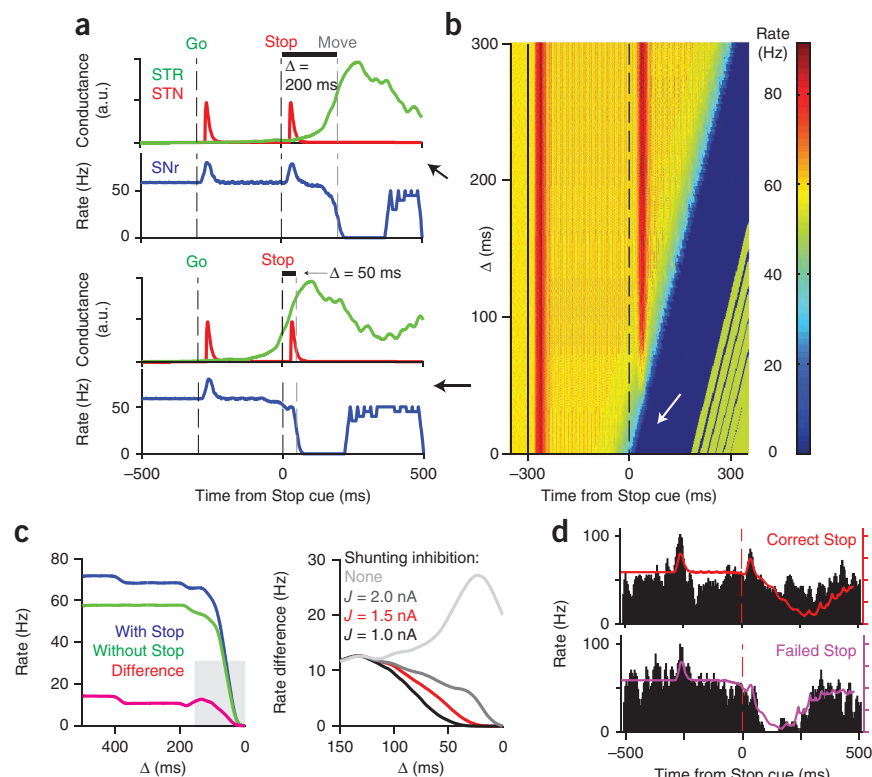
DISCUSSION

Race models have been central to theories of action suppression for decades, yet clear evidence that they actually describe neural processes has been elusive. Here we demonstrated that activity in two key basal ganglia pathways for action control closely resembles a race between go and stop processes. Individual SNr neurons exhibited both movement-related pauses in firing (driven by striatum) and rapid increases in firing rate after Stop cues (driven by STN), and the relative timing of these influences corresponded to whether stopping was successful. These SNr cells are located in a specific dorsolateral subregion, that projects to collicular intermediate layers important for the control of orienting movements[25,26]. Furthermore, the evidence we found for shunting inhibition of STN inputs by striatal inputs begins to reveal how mechanisms operating in single cells can contribute to sensorimotor gating.

Neurons in STN and SNr with fast Stop cue responses also increased spiking with the Go cue that instructed contralateral movement (**Supplementary Figs. 3** and **8**). Thus, the STN-SNr pathway does not solely convey signals that instruct stopping but also other task-relevant cues. The effect of both Go and Stop cues was to transiently increase firing of a population of SNr neurons that decrease firing with the onset of movement. We found that trials in which STN and SNr responded more strongly to the Go cue had longer reaction times (**Supplementary Fig. 9**), consistent with a role for STN-SNr transmission in delaying behavioral output[2] rather than causing outright stopping (see below). A rapid, 'automatic' inhibition of behavioral responses by task-relevant cues may help prevent responses that are impulsive or premature (that is, when preparation for movement is incomplete) and also explain why even cues that instruct subjects not to stop but instead continue as planned result in longer reaction times[36].

Our results contribute information to the ongoing debate about whether certain brain areas contribute to action inhibition versus cue-evoked reorienting of attention[36–38], indicating that these functions are not necessarily distinct.

The very low, fixed latency of cue-evoked activity in STN is informative in several ways. First, race models often incorporate variable timing of both go and stop processes, yet we found that the STN response to the Stop cue occurred at the same time in Correct and Failed Stop trials. Thus, if these responses are part of a stop process, performance variability arises directly from the variable timing of the go process (corresponding to variable reaction times), at least in this version of the stop-signal task. This result is consistent with recent simulations of basal ganglia networks during inhibitory control[39]: STN provides the same fast signal to pause action, whether stopping is actually successful or not.

Second, increased STN spiking within just 15 ms of the onset of a cue constrains the sophistication of prior information processing, and which afferents can drive this response. Recent studies in humans have emphasized the role of frontal cortical inputs to STN in action suppression[1,14], but it is not clear that cue information can be passed quickly enough through cortex to cause this fast STN spiking. Our implementation of the stop-signal task encouraged very quick responses and may have increased the importance of subcortical pathways that support sensory processing and fast orienting-like movements. In particular, many neurons in the thalamic intralaminar complex (centromedian and parafascicular nuclei, CM-Pf) and pedunculopontine nucleus have short-latency responses to salient auditory stimuli[40,41] and project to a range of basal ganglia targets, including the STN[42,43]. CM-Pf projections to striatum are important for behavioral switching and learning after unexpected cues[44–46].

We hypothesize that the STN responses we observed are one component of a broader 'interrupt' system, mediated by CM-Pf and/or pedunculopontine nucleus, that coordinates a response to salient cues across multiple timescales using multiple pathways (**Supplementary Fig. 10**). In this scheme, very fast yet transient excitation of STN and SNr serves to delay actions that are close to execution, similar to previous descriptions of STN 'buying time' during decision-making[47].

However, the STN-driven increase in SNr firing is highly transient; in our simulation it delayed, but did not fully cancel, the striatum-driven decrease in firing that releases movements (**Fig. 6e**). We also found evidence that a second, slower mechanism may act in the striatum to help shut down the go process. Movement-related striatal activity abruptly decreased in Correct Stop trials, compared to Slow Go trials (**Fig. 5b,c** and **Supplementary Fig. 6**), and a similar suppression of contralateral-coding striatal activity has been observed in an antisaccade task[48]. Such suppression of a go process is a key feature of 'interactive race' models of stop-signal performance[4]. Yet striatum-based processing by itself is unlikely to account for stop-signal performance, as the reduction in striatal output was not consistently before the SSRT (**Fig. 5c**). It thus appears that complementary mechanisms allow action suppression to be both fast (via STN) and selective (via striatum)[19,39,48]. Future studies will investigate how the striatal go process is suppressed in Correct Stop trials. Direct pathway neurons can be inhibited in many ways, and some (non-exclusive) possibilities include the influences of indirect pathway cells[39,48,49] and cholinergic interneurons[40,46].

We used a basic stop-signal task, designed to investigate 'reactive' aspects of behavioral inhibition (responding to a Stop cue). This task does not assess all the complexities of behavioral inhibition, such as 'proactive' components (that is, preparedness to stop). It has been proposed that proactive inhibition involves yet another basal ganglia circuit, the indirect pathway from striatum[50] through globus pallidus[19]. In follow-up studies, we plan to investigate whether systematically varying preparedness to stop reveals a clear role for globus pallidus that was not apparent here.

Finally, we had previously reported[21] (using the experiment 1 data) that salient task cues cause a rapid reset of beta oscillatory phase throughout the basal ganglia, whether or not the cues actually direct behavior on a given trial. By contrast, cue-induced increases in beta power only occur for cues that are 'used', for example, after the Stop cue on Correct but not Failed Stop trials. This distinction corresponds closely to the difference between STN and SNr described here: events that caused abrupt increases in STN firing also produced restet of beta phase, whereas those events that additionally increased SNr firing subsequently produced increases in beta power. Furthermore, there is evidence that other oscillatory frequencies such as delta and theta can influence the parameters of behavioral control, such as decision thresholds[47]. An important direction for future investigation will be to determine the mechanistic relationships between rapid firing rate changes and altered dynamic states in basal ganglia circuitry.

METHODS
Methods and any associated references are available in the online version of the paper.

Note: Supplementary information is available in the online version of the paper.

AUTHOR CONTRIBUTIONS
J.D.B. designed and oversaw the project. D.K.L. helped develop the behavioral task. D.K.L., N.M. and F.C. performed electrophysiological experiments. R.S. developed and performed the data analyses and computational modeling. R.S. and J.D.B. wrote the manuscript.

1. Aron, A.R. & Poldrack, R.A. Cortical and subcortical contributions to Stop signal response inhibition: role of the subthalamic nucleus. *J. Neurosci.* **26**, 2424–2433 (2006).
2. Frank, M.J. Hold your horses: a dynamic computational role for the subthalamic nucleus in decision making. *Neural Netw.* **19**, 1120–1136 (2006).
3. Logan, G.D., Cowan, W.B. & Davis, K.A. On the ability to inhibit simple and choice reaction time responses: a model and a method. *J. Exp. Psychol. Hum. Percept. Perform.* **10**, 276–291 (1984).
4. Boucher, L., Palmeri, T.J., Logan, G.D. & Schall, J.D. Inhibitory control in mind and brain: an interactive race model of countermanding saccades. *Psychol. Rev.* **114**, 376–397 (2007).
5. Robbins, T.W., Gillan, C.M., Smith, D.G., de Wit, S. & Ersche, K.D. Neurocognitive endophenotypes of impulsivity and compulsivity: towards dimensional psychiatry. *Trends Cogn. Sci.* **16**, 81–91 (2012).
6. Eagle, D.M. *et al.* Stop-signal reaction-time task performance: role of prefrontal cortex and subthalamic nucleus. *Cereb. Cortex* **18**, 178–188 (2008).
7. Hanes, D.P. & Schall, J.D. Neural control of voluntary movement initiation. *Science* **274**, 427–430 (1996).
8. Osman, A., Kornblum, S. & Meyer, D.E. The point-of-no-return in choice reaction-time–controlled and ballistic stages of response preparation. *J. Exp. Psychol. Hum. Percept. Perform.* **12**, 243–258 (1986).
9. Hikosaka, O. & Wurtz, R.H. Effects on eye-movements of a GABA agonist and antagonist injected into monkey superior colliculus. *Brain Res.* **272**, 368–372 (1983).
10. Baunez, C. *et al.* Effects of STN lesions on simple vs choice reaction time tasks in the rat: preserved motor readiness, but impaired response selection. *Eur. J. Neurosci.* **13**, 1609–1616 (2001).
11. Bergman, H., Wichmann, T. & DeLong, M.R. Reversal of experimental parkinsonism by lesions of the subthalamic nucleus. *Science* **249**, 1436–1438 (1990).
12. Ballanger, B. *et al.* Stimulation of the subthalamic nucleus and impulsivity: release your horses. *Ann. Neurol.* **66**, 817–824 (2009).
13. Majid, D.S., Cai, W., George, J.S., Verbruggen, F. & Aron, A.R. Transcranial magnetic stimulation reveals dissociable mechanisms for global versus selective corticomotor suppression underlying the stopping of action. *Cereb. Cortex* **22**, 363–371 (2012).
14. Jahfari, S. *et al.* Effective connectivity reveals important roles for both the hyperdirect (fronto-subthalamic) and the indirect (fronto-striatal-pallidal) fronto-basal ganglia pathways during response inhibition. *J. Neurosci.* **31**, 6891–6899 (2011).
15. Frank, M.J., Samanta, J., Moustafa, A.A. & Sherman, S.J. Hold your horses: impulsivity, deep brain stimulation, and medication in parkinsonism. *Science* **318**, 1309–1312 (2007).
16. Hikosaka, O. & Wurtz, R.H. Visual and oculomotor functions of monkey substantia nigra pars reticulata. I. Relation of visual and auditory responses to saccades. *J. Neurophysiol.* **49**, 1230–1253 (1983).
17. Kravitz, A.V. *et al.* Regulation of parkinsonian motor behaviours by optogenetic control of basal ganglia circuitry. *Nature* **466**, 622–626 (2010).
18. Bevan, M.D., Bolam, J.P. & Crossman, A.R. Convergent synaptic input from the neostriatum and the subthalamus onto identified nigrothalamic neurons in the rat. *Eur. J. Neurosci.* **6**, 320–334 (1994).
19. Aron, A.R. From reactive to proactive and selective control: developing a richer model for stopping inappropriate responses. *Biol. Psychiatry* **69**, e55–e68 (2011).
20. Gage, G.J., Stoetzner, C.R., Wiltschko, A.B. & Berke, J.D. Selective activation of striatal fast-spiking interneurons during choice execution. *Neuron* **67**, 466–479 (2010).
21. Leventhal, D.L. *et al.* Basal ganglia beta oscillations accompany cue utilization. *Neuron* **73**, 523–536 (2012).
22. Stuphorn, V., Brown, J.W. & Schall, J.D. Role of supplementary eye field in saccade initiation: executive, not direct, control. *J. Neurophysiol.* **103**, 801–816 (2010).
23. Brown, J.W., Hanes, D.P., Schall, J.D. & Stuphorn, V. Relation of frontal eye field activity to saccade initiation during a countermanding task. *Exp. Brain Res.* **190**, 135–151 (2008).

24. Cheruel, F., Dormont, J.F. & Farin, D. Activity of neurons of the subthalamic nucleus in relation to motor performance in the cat. *Exp. Brain Res.* **108**, 206–220 (1996).
25. Deniau, J.M., Mailly, P., Maurice, N. & Charpier, S. The pars reticulata of the substantia nigra: a window to basal ganglia output. *Prog. Brain Res.* **160**, 151–172 (2007).
26. Pare, M. & Hanes, D.P. Controlled movement processing: superior colliculus activity associated with countermanded saccades. *J. Neurosci.* **23**, 6480–6489 (2003).
27. Handel, A. & Glimcher, P.W. Quantitative analysis of substantia nigra pars reticulata activity during a visually guided saccade task. *J. Neurophysiol.* **82**, 3458–3475 (1999).
28. Schultz, W. Activity of pars reticulata neurons of monkey substantia-nigra in relation to motor, sensory, and complex events. *J. Neurophysiol.* **55**, 660–677 (1986).
29. Basso, M.A. & Sommer, M.A. Exploring the role of the substantia nigra pars reticulata in eye movements. *Neuroscience* **198**, 205–212 (2011).
30. Albin, R.L., Young, A.B. & Penney, J.B. The functional-anatomy of basal ganglia disorders. *Trends Neurosci.* **12**, 366–375 (1989).
31. Lo, C.C. & Wang, X.J. Cortico-basal ganglia circuit mechanism for a decision threshold in reaction time tasks. *Nat. Neurosci.* **9**, 956–963 (2006).
32. Humphries, M.D. & Gurney, K.N. A pulsed neural network model of bursting in the basal ganglia. *Neural Netw.* **14**, 845–863 (2001).
33. Humphries, M.D., Stewart, R.D. & Gurney, K.N. A physiologically plausible model of action selection and oscillatory activity in the basal ganglia. *J. Neurosci.* **26**, 12921–12942 (2006).
34. Blomfield, S. Arithmetical operations performed by nerve cells. *Brain Res.* **69**, 115–124 (1974).
35. Segev, I. Dendritic processing. in *The Handbook of Brain Theory and Neural Networks*. (ed. Arbib, M.A.) 282–289 (MIT Press, 1998).
36. Sharp, D.J. *et al.* Distinct frontal systems for response inhibition, attentional capture, and error processing. *Proc. Natl. Acad. Sci. USA* **107**, 6106–6111 (2010).
37. Shulman, G.L. *et al.* Interaction of stimulus-driven reorienting and expectation in ventral and dorsal frontoparietal and basal ganglia-cortical networks. *J. Neurosci.* **29**, 4392–4407 (2009).
38. Levy, B.J. & Wagner, A.D. Cognitive control and right ventrolateral prefrontal cortex: reflexive reorienting, motor inhibition, and action updating. *Ann. NY Acad. Sci.* **1224**, 40–62 (2011).
39. Wiecki, T.V. & Frank, M.J. A computational model of inhibitory control in frontal cortex and basal ganglia. *Psychol. Rev.* **120**, 329–355 (2013).
40. Matsumoto, N., Minamimoto, T., Graybiel, A.M. & Kimura, M. Neurons in the thalamic CM-Pf complex supply striatal neurons with information about behaviorally significant sensory events. *J. Neurophysiol.* **85**, 960–976 (2001).
41. Pan, W.X. & Hyland, B.I. Pedunculopontine tegmental nucleus controls conditioned responses of midbrain dopamine neurons in behaving rats. *J. Neurosci.* **25**, 4725–4732 (2005).
42. Deschenes, M., Bourassa, J., Doan, V.D. & Parent, A. A single-cell study of the axonal projections arising from the posterior intralaminar thalamic nuclei in the rat. *Eur. J. Neurosci.* **8**, 329–343 (1996).
43. Kita, T. & Kita, H. Cholinergic and non-cholinergic mesopontine tegmental neurons projecting to the subthalamic nucleus in the rat. *Eur. J. Neurosci.* **33**, 433–443 (2011).
44. Kimura, M., Minamimoto, T., Matsumoto, N. & Hori, Y. Monitoring and switching of cortico-basal ganglia loop functions by the thalamo-striatal system. *Neurosci. Res.* **48**, 355–360 (2004).
45. McHaffie, J.G., Stanford, T.R., Stein, B.E., Coizet, W. & Redgrave, P. Subcortical loops through the basal ganglia. *Trends Neurosci.* **28**, 401–407 (2005).
46. Ding, J.B., Guzman, J.N., Peterson, J.D., Goldberg, J.A. & Surmeier, D.J. Thalamic gating of corticostriatal signaling by cholinergic interneurons. *Neuron* **67**, 294–307 (2010).
47. Cavanagh, J.F. *et al.* Subthalamic nucleus stimulation reverses mediofrontal influence over decision threshold. *Nat. Neurosci.* **14**, 1462–1467 (2011).
48. Watanabe, M. & Munoz, D.P. Neural correlates of conflict resolution between automatic and volitional actions by basal ganglia. *Eur. J. Neurosci.* **30**, 2165–2176 (2009).
49. Cui, G. *et al.* Concurrent activation of striatal direct and indirect pathways during action initiation. *Nature* **494**, 238–242 (2013).
50. Zandbelt, B.B. & Vink, M. On the role of the striatum in response inhibition. *PLoS ONE* **5**, e13848 (2010).
51. Paxinos, G. & Watson, C. *The Rat Brain in Stereotaxic Coordinates* 5th edn. (Elsevier Academic Press, 2005).

ONLINE METHODS

Experimental procedures. Behavioral electrophysiology methods have been previously described in detail[20,21,52]. All animal experiments were approved by the University of Michigan Committee for the Use and Care of Animals. Subjects were adult male Long-Evans rats, housed on a 12:12 reverse light:dark cycle and tested during the dark phase. Rats were housed in groups of 3–4 with moderate environmental enrichment (toys, variety of bedding, 59 cm × 39 cm × 20 cm cages) during presurgical training, then were singly housed after surgery. The operant chamber had five nose-poke holes on one wall and a food dispenser on the opposite wall. At the start of each trial, one of the three more-central holes (chosen randomly) was illuminated, indicating that the rat should poke and hold its nose in that port. After a variable hold delay (500–1,200 ms), a tone (Go cue; 65 dB, 50 ms) instructed the rat to move promptly into the adjacent hole either to the left (1-kHz tone) or right (4-kHz tone); correct choices triggered immediate delivery of a sugar pellet reward (signaled by an audible click of the food dispenser). To encourage rats to respond quickly, on Go trials rats had to leave the initial port within a 'limited hold' period, and then poke the adjacent hole within a 'movement hold' (**Supplementary Table 1**). On Stop trials (30%), the Go cue was followed after a short delay (the stop-signal delay, SSD) by a Stop cue (white noise burst, 65 dB, 125 ms). If the rat moved before the SSD, the Stop cue was not played and the trial was treated as a Go trial. To successfully complete a Stop trial, the rat had to maintain its nose in the initial port until the limited hold period would have expired on a Go trial. At that point, the audible click of the food dispenser signaled reward delivery. Errors of any type produced a time-out (house light on for 8 s). Otherwise, the next trial was initiated after the rat obtained its reward. The computer-controlled sequence of trials was randomized and experimenters were blinded to the trial sequence. However, to further discourage the rat from adopting a holding strategy, the rat had to perform a correct Go trial before a Stop trial could occur. Other randomization or blinding procedures were not performed in this study.

After achieving stable task performance (typically ~2–3 months of training, >70% correct choices on Go trials) rats in experiment 1 received implants containing 21 individually drivable tetrodes targeting basal ganglia structures (striatum (STR), globus pallidus, STN and SNr), and recording sessions began ~1 week later. SSD was held constant in each recording session to facilitate electrophysiological analyses but was adjusted between stop-signal sessions so that Correct and Failed Stop trials were approximately equal in number. On alternate days, rats performed the stop-signal task and a go/no-go task, which was identical in most respects to the stop-signal task but with an SSD of zero (on No-Go trials, the white noise was played instead of a Go cue). During task performance, wide-band (1–9,000 Hz) brain signals were recorded continuously at 31.25 kHz. Tetrodes were usually moved by at least 80 μm between two stop-signal sessions. In some cases (for example, if the number of trials was low in one recording session), tetrodes were not moved between sessions, and we only included the better session in the analysis. Individual neurons were isolated offline using wavelet-based filtering[52] followed by standard manual spike-sorting, and classification into different presumed cell types[53]. No statistical methods were used to predetermine sample sizes.

In experiment 2 we examined whether stop responses are localized to a specific subregion of SNr. To facilitate a systematic functional mapping, three rats received 8-shank, 64-channel silicon probes (Neuronexus Inc.) in the SNr. Silicon probe shanks were coated in the lipophilic dye DiO before implantation and not moved after initial surgery. For these fixed-location silicon probes we only included data from a single session per rat, to avoid including duplicate cells. Two additional rats received similar tetrode implants as in experiment 1. Locations of SNr single units were reconstructed on the published SNr coronal atlas boundaries[51].

Data analysis. All analyses were performed using custom Matlab routines. Data distribution was not formally tested for normality, but we instead mostly used statistical methods that are robust for non-normal-distributed data (Kolmogorov-Smirnov and shuffling tests). SSRTs were estimated for each session individually by the integration method[54], as follows. First, we determined the percentage of Failed Stop trials f. Then we calculated the stopping time as the f-th percentile of the distribution of Go trial reaction times. The SSRT is then the stopping time minus the SSD[54]. This SSRT value was also used to separate Go trials in the same session into 'Fast Go' and 'Slow Go'.

To examine the activity of each neuron we used 40-ms time bins (sliding in steps of 20 ms) to obtain spike-count distributions for different trial types, near

key task events. A neuron had to exceed a 3-Hz firing rate in at least one time bin to be included in subsequent analyses. To best isolate activity associated with Stop cues, we compared trial types for which the activity associated with movement preparation is most similar. That is, we compared Failed Stop trials with Fast Go trials, and Correct Stop trials with Slow Go trials[22,23] (latency matching). For Stop trials, neural activity was aligned to the onset of the Stop cue, and for Go trials, we used the time at which the Stop signal would have occurred, that is, Go cue onset + SSD. For a few Failed Stop trials, reaction times were very long (**Fig. 1d**). We interpreted these as trials for which the initial stopping was actually successful but subsequent holding on for reward was not (both spike and LFP measures were consistent with this interpretation; data not shown). We therefore excluded Failed Stop trials with reaction times >500 ms from all analyses.

To compare whether spike rates were different between two trial types, we used a shuffle test for each time bin. We shuffled the trial type labels 10,000 times, and for each shuffle we compared the means of the two resulting spike count distributions. To obtain a P value, we determined the fraction of shuffles in which the difference between the shuffled means was larger (or smaller) than the difference between the two actually observed means. We used a P value of 0.05 to determine significant coding of trial types. It follows that 5% of a population of randomly active units should, on average, be classified as 'coding' (all false positives). A binomial test was then used to determine whether the empirically measured fraction of coding units was significantly higher than that expected by chance. We corrected for multiple testing with respect to the overall time-window around task events (for example, for **Fig. 2**, each single test was done for a 40-ms time window, yielding 500/40 independent tests around the task events). This correction is overly conservative for some key time points of interest, as we hypothesized a priori that firing-rates would change shortly after cue onset. Therefore we also (in **Fig. 2a**) indicated times when the P value was below 0.05 without adjusting for multiple comparisons.

The analyses shown in **Figure 3** include only STN and SNr units identified as 'stop-related'. For STN, we included units that contributed to the significant responses in either Correct or Failed Stop trials (filled red and magenta bars for STN in **Fig. 2a**). As the overall population of SNr units did not reach significance in Failed Stop trials, we included only those individual SNr units that contributed to the significant Stop cue response in Correct Stop trials (filled red bars for SNr in **Fig. 2a**). The firing rate time course of each unit was then estimated by averaging spike counts over trials of the same type (for example, Failed Stop right trials) with a sliding 20 ms window in steps of 5 ms around important task events (for example, the Stop cue; **Fig. 4a**), and then smoothing with a three-point average. To compare mean firing rate time courses between trial types, activity of each unit was first transformed to z scores using the mean and s.d. of session-wide firing rate estimates (obtained from 1-s-wide windows). To compare the magnitude of the Stop cue response between Correct and Failed Stop trials (**Fig. 3c**), we used peak firing rates in the range 10–70 ms after onset of Stop cue. To more precisely identify the times at which STN and SNr neurons responded to the Stop cue (**Fig. 3b**), we used non-overlapping 3-ms time windows smoothed with a three-point average for the firing rate estimation. The latency was taken as the time of peak firing within the range 10–70 ms after onset of Stop cue. Units were marked in red (in **Fig. 4** and **Supplementary Fig. 4a–d**) if the corresponding trial types were significantly different in at least two out three bins (each bin was 40 ms wide, centered at 40, 60 and 80 ms after the stop cue). For the data shown in **Figure 4**, we compared trial types separately for ipsilateral and contralateral conditions and marked units red if in one or both cases the activity differences were significant. Similarly, in **Supplementary Figure 2b**, a unit was counted in the histogram if it exhibited a significant difference in activity between Failed and Correct Stop trials for ipsilateral or contralateral trials.

Computational modeling. To describe the gating of the Stop cue response, we implemented an integrate-and-fire model of a single SNr cell. Changes in the membrane potential V at time t were given by[46]

$$\tau_{\mathrm{m}} \frac{dV}{dt} = -V(t) + E_{\mathrm{m}} - r_{\mathrm{m}}I(t)$$

where τ_{m} is the membrane time constant, E_{m} the membrane resting potential, and r_{m} the membrane input resistance. I is a sum of currents: $I(t) = I_{\mathrm{b}}(t) + I_{\mathrm{STR}}(t) + I_{\mathrm{STN}}(t)$. The current I_{b} was used to mimic the high spontaneous activity observed in SNr cells: $I_{\mathrm{b}}(t) = g_{\mathrm{b}}(V(t) - E_{\mathrm{b}})$ (see below for parameter settings)[32,55]. Synaptic

input from the striatum was summarized by $I_{STR}(t) = g_{STR}(t)(V(t)-E_{STR})$. The time-dependent synaptic conductance $g_{STR}(t)$ was modeled using the activity $a(t)$ of go-related striatal cells during movement initiation shown in **Figure 5b** on the right, averaged over slow and Fast Go trials, as:

$$g_{STR}(t) = \eta a(t)\sum_{i=0}^{t} a(i)$$

The scaling factor η controls the movement-related decrease in our model SNr cell and was fitted to reproduce the average time course in **Supplementary Figure 4**. This provided an important constraint on the overall strength of striatal inhibition. Although further increases in striatal input strength could block STN inputs without the need for shunting inhibition, this change also produced too early a pause in SNr firing (that is, a mismatch with the timing of striatal and SNr changes observed *in vivo*). The sum $\sum_{i=0}^{t} a(i)$ is over previous activity in the current trial (starting 500 ms before onset of movement) and is used as a simplified description of facilitation found at striatonigral synapses[56]. In our model this facilitation effectively lead to a broader peak of the striatal activity ramp and thereby to a broader pause in SNr activity, as we observed in the experimental data. Although real SNr neurons pause at a range of times relative to the onset of movement (**Supplementary Fig. 3** and ref. 29), for our simple model we used a fixed striatal input time course. We further assumed that STN input to SNr consisted of a single spike at time t_s evoked by the Go or Stop cue (see STN example cell in **Fig. 2b**). Each spike gave rise to a modulated alpha function[55] yielding a synaptic current $I_{STN}(t) = vh(t)\alpha(t,t_s)(V(t)-E_{STN})$ with a scaling factor v and a shunting factor $h(t)$. The scaling factor v controls the amplitude of the SNr response to the STN input. We choose v to fit the amplitude of SNr responses to the Go cue. Owing to the high baseline activity in SNr mediated by I_b, in some trials STN inputs can shift the spike timing rather than increase the SNr firing rate. When the SNr baseline activity is diminished by inhibitory input, this effect is diminished so that STN input becomes more likely to evoke an SNr spike (gray line in **Fig. 6c** on the right). The alpha function was zero for $t < 0$ and otherwise defined as $\alpha(t,t_s) = \exp(-(t-t_s)/q) - \exp(-(t-t_s)/0.25q)$ with a time constant q. The shunting factor $h(t)$ takes values between zero and one depending on the amount of inhibitory current[32,33]:

$$h(t) = \left(1 - \frac{I_{STR}(t)}{J}\right)\Theta\left(1 - \frac{I_{STR}(t)}{J}\right),$$

where Θ denotes the Heaviside step function. The reference current J controls the efficacy of the shunting inhibition (**Fig. 6c**).

A spike was generated by the model SNr cell if $V(t)$ reached the threshold voltage $V_{thr} = -50$ mV. After one millisecond, $V(t)$ was then reset to the equilibrium membrane potential $E_m = -80$ mV. Other parameter values were $\tau_m = 20$ ms; $r_m = 10$ MΩ; $g_b = 0.095$ μS; $E_b = 0$ mV; $E_{STR} = -100$ mV; $E_{STN} = 0$ mV; $\eta = 1/1,200$; $v = 0.1$; $q = 10$ ms; and $J = 1$ nA, 1.5 nA and 2 nA for 'strong', 'medium' and 'weak' shunting inhibition, respectively. Further, complex effects on synaptic integration of GABA$_A$ were neglected in our model as for simplicity we set $E_{STR} < E_m$.

However, we performed additional simulations with more realistic values for shunting inhibition where $E_m < E_{STR} < V_{thr}$. With appropriately rescaled values for η and J, the results remained the same. Therefore, the key feature of inhibition was the divisive 'vetoing' effect[34,35] on excitatory STN input. For the simulation without shunting inhibition $h(t)$ was always set to 1.

In the model we kept the SSD constant at 300 ms, and assumed that STN input reached SNr starting 30 ms after Stop cue onset. The SNr response to the Stop cue was measured as the firing rate within the subsequent 50-ms time window. The interval Δ between presentation of Stop cue and onset of movement was varied in 1-ms time steps, over the range of 0–500 ms. For each Δ, 500 trials with and 500 trials without the Stop cue were simulated and the average firing rates were then used for the results.

To obtain SNr output for Failed Stop trials, we used the behavioral data of the rats. From the measured reaction times of Failed Stop trials, we subtracted the SSD for that session. The resulting distribution of Stop-aligned reaction times (**Supplementary Fig. 7**) was used as the model parameter Δ for Failed Stop trials.

For Correct Stop trials, no direct reaction time measure is available. However, using the reaction time distribution on Go trials, it is possible to estimate what the reaction time would have been if the Stop cue had not been presented. More formally, for each rat we had an empirically measured reaction time distribution for Go trials $F_{go}(t) = P(RT = t)$, with P denoting probability and RT being Stop-aligned reaction times in 50-ms-wide bins. With the corresponding probability distribution for Failed Stop trials F_{FS}, the hypothetical distribution of correct stop reaction times was estimated as

$$F_{CS}(t) = \frac{F_{Go}(t) - pF_{FS}(t)}{1 - p}$$

where p denotes the overall probability of failing to stop (number of Failed Stop trials divided by the number of Stop trials). Owing to noise in the behavioral data in a few cases the estimates of F_{CS} were negative, so we applied a lower bound for $F_{CS}(t)$ of zero and rescaled the whole probability distribution to maintain a total probability of 1. The resulting estimates of F_{CS} were then used as the distribution of Δ for Correct Stop trials.

52. Wiltschko, A.B., Gage, G.J. & Berke, J.D. Wavelet filtering before spike detection preserves waveform shape and enhances single-unit discrimination. *J. Neurosci. Methods* **173**, 34–40 (2008).
53. Berke, J.D. Uncoordinated firing rate changes of striatal fast-spiking interneurons during behavioral task performance. *J. Neurosci.* **28**, 10075–10080 (2008).
54. Verbruggen, F. & Logan, G.D. Models of response inhibition in the stop-signal and stop-change paradigms. *Neurosci. Biobehav. Rev.* **33**, 647–661 (2009).
55. Gerstner, W. & Kistler, W.M. *Spiking Neuron Models* (Cambridge University Press, 2002).
56. Connelly, W.M., Schulz, J.M., Lees, G. & Reynolds, J.N.J. Differential short-term plasticity at convergent inhibitory synapses to the substantia nigra pars reticulata. *J. Neurosci.* **30**, 14854–14861 (2010).